



FLEXURAL PERFORMANCE OF SLENDER HIGH STRENGTH STEEL FIBER REINFORCED CONCRETE COLUMNS UNDER AXIAL AND LATERAL LOADINGS

Y. Tanabe⁽¹⁾, Y. Ishikawa⁽²⁾

⁽¹⁾ Takenaka Corporation, Research & Development Institute, Researcher, M.Eng, tanabe.yuusuke@takenaka.co.jp

⁽²⁾ Takenaka Corporation, Research & Development Institute, Chief Researcher, Dr.Eng, ishikawa.yuuji@takenaka.co.jp

...

Abstract

This paper describes an experimental study conducted on slender columns made of Steel Fiber Reinforced Concrete (SFRC). By using high strength concrete and high strength steel bars, the cross section of these slender SFRC columns is reduced to 1/4 that of columns made of ordinary concrete. The slender ratio (height to diameter ratio) of these columns is about 10 or higher. The SFRC contains 0.6% volume fraction of high strength steel fibers. The compressive strength of SFRC ranges from 172 to 234 N/mm² and tensile strength of steel bars ranges from 295 to 980 N/mm². Lateral loading tests are carried out to investigate the flexural performance of these columns. The experimental parameters are the compressive strength, size of column section, number and strength of steel bars, and contents of steel fibers. The test results show that using steel fiber decreases the damage of cover concrete of the columns and increases their flexural strength. In addition, the results show that slender SFRC columns possess high drift capacity. Several standards are used to evaluate the strength of the tested slender columns. The stress block factors relative to high strength concrete given in the New Zealand standard allow a good strength estimation of these columns. The impact of several parameters on the flexural strength evaluation is also presented.

Keywords: High Strength Steel Fiber Reinforced Concrete, Slender Column, Flexural Strength

1. Introduction

Along with the increase in constructions of high rise buildings, the development of high strength concrete has considerably progressed [1]-[4]. In the 1980s, many studies on high strength concrete of 100 N/mm² grade had been made, in Japan [5]-[7]. Recently, ultra-high strength concrete of compressive strength over 150 N/mm² has been developed and applied to columns which would bear high axial force levels, such as columns of lower floors in high rise buildings. For example, 150 N/mm² concrete was applied in the first floor columns of a 59-story apartment building and in the CFT columns of a 300m-high multi-purpose building. Furthermore, because there are more demands for larger spaces, even in low-rise buildings, reduction of the cross section area of columns is required. Therefore, as Japan is a highly seismic country and for the purpose of examining the structural performance of slender columns using ultra-high strength concrete, experiments were carried out on such columns under axial and lateral loads. These columns are not only axial force support columns but also would present flexural moment resistance, as they are expected to have fixed ends. Ultra-high strength concrete that has substantially a linear behavior until reaching its maximum strength (Fig. 1) and ranging from 172 to 234 N/mm², was used. Steel fibers (Fig. 2) were added to the concrete in order to prevent a brittle fracture of such high strength concrete under large compression stresses. In addition, high strength steel bars were applied in the columns to stand high level axial forces.

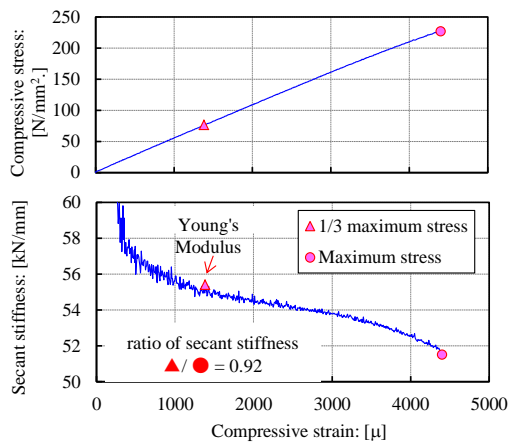


Fig. 1 – Characteristics of ultra-high strength concrete

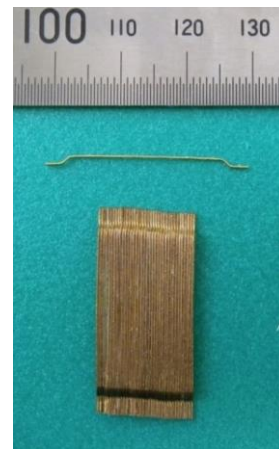


Fig. 2 – Steel Fibers

2. Outline of Experiment

2.1 Outline of specimens

Table 1 shows the characteristics of the specimens and Fig. 3 shows their elevation and cross sections. The constructed specimens were of full scale. Experiments were carried out on three series. Series 1 contained three specimens, where the parameters were the shape and amount of steel fibers. Series 2 contained four specimens, where the parameters were the compressive strength of concrete, cross section, and characteristics of steel bars. The single specimen in Series 3 had steel bars of normal strength. Each specimen was composed of a column part, two stubs and a gap of 20 mm at each column end, which was filled with high-strength grout. Longitudinal steel bars of the column were mechanically bonded to the stubs using mechanical joints and high-strength grout. The compressive strength of the grout ranged from 180 to 200 N/mm².

(1) Series 1

In Series 1, the concrete strength was about 220N/mm². Specimen SFC01 had a circular cross section of 200 mm diameter. Specimens SFC02 and SNC03 had rectangular cross sections of 150 x 250 mm size. The height to diameter ratio (h/D) of SFC01 was 11.7, while the one of SFC02 and SNC03 was 9.36. Concrete of SFC01 and

SFC02 contained steel fibers with a volume ratio $V_f = 0.6 \text{ Vol.}\%$ and that of SNC03 did not. Steel fibers were of mixed types. Their diameter was 0.38 mm, their length was 30 mm resulting in an aspect ratio of 79, and their tensile strength was higher than 3070 N/mm^2 . The specific strength of SD980 main bars was 980 N/mm^2 , and the one of SD785 hoops was 785 N/mm^2 .

(2) Series 2

In Series 2, the concrete strength of SFC04 and SFC05 was about 170 N/mm^2 . The specimen's diameter was 350 mm. SFC04 had six main bars of D22 (SD590) while SFC05 had four main bars of the same diameter and type. The concrete strength of SFC06 and SFC07 was about 210 N/mm^2 . The specimen's diameter was 300 mm. While SFC06 had six main bars of D19 (SD685), SFC07 had four main bars of the same diameter and type and another thick bar of D25 (SD685) at the column's center. The height of columns in this series was 3450mm, and their h/D was 9.86 and 11.5. The hoops were of spiral shape and of U10.7 (SBPD1275) type.

Table 1 – Attributes of specimens

Series	Specimen	Cross section [mm]	Height [mm] (ratio h/D)	Concrete strength f_c [N/mm^2]	Axial force [kN] (ratio η)	Fiber ratio V_f [Vol.%]	Main bar (ratio p_g)	Hoop (ratio p_w)
1	SFC01	○ 200φ	2340 (11.7)	214	1650 (0.25)	0.6	6-D16, SD980 ($p_g=3.80\%$)	S6@50, KSS785 ($p_w=0.62\%$)
	SFC02	□ 150 x 250	2340 (9.36)	214	2000 (0.25)	0.6	4-D16, SD980 ($p_g=2.12\%$)	S6@50, KSS785 ($p_w=0.83\%$)
	SNC03	□ 150 x 250	2340 (9.36)	234	2000 (0.23)	0.0	4-D16, SD980 ($p_g=2.12\%$)	S6@50, KSS785 ($p_w=0.83\%$)
2	SFC04	○ 350φ	3450 (9.86)	172	4350 (0.26)	0.6	6-D22, SD590 ($p_g=2.42\%$)	U10.7@90, SBPD1275 ($p_w=0.57\%$)
	SFC05	○ 350φ	3450 (9.86)	172	4350 (0.26)	0.6	4-D22, SD590 ($p_g=1.61\%$)	U10.7@90, SBPD1275 ($p_w=0.57\%$)
	SFC06	○ 300φ	3450 (11.5)	207	4250 (0.29)	0.6	6-D19, SD685 ($p_g=2.41\%$)	U10.7@105, SBPD1275 ($p_w=0.67\%$)
	SFC07	○ 300φ	3450 (11.5)	207	4250 (0.29)	0.6	4-D19, SD685 ($p_g=1.60\%$)	U10.7@105, SBPD1275 ($p_w=0.67\%$)
3	SFC08	○ 250φ	2485 (9.94)	234	3420 (0.30)	0.6	4-D16, SD295 ($p_g=1.60\%$)	φ6@100, SR295 ($p_w=0.67\%$)

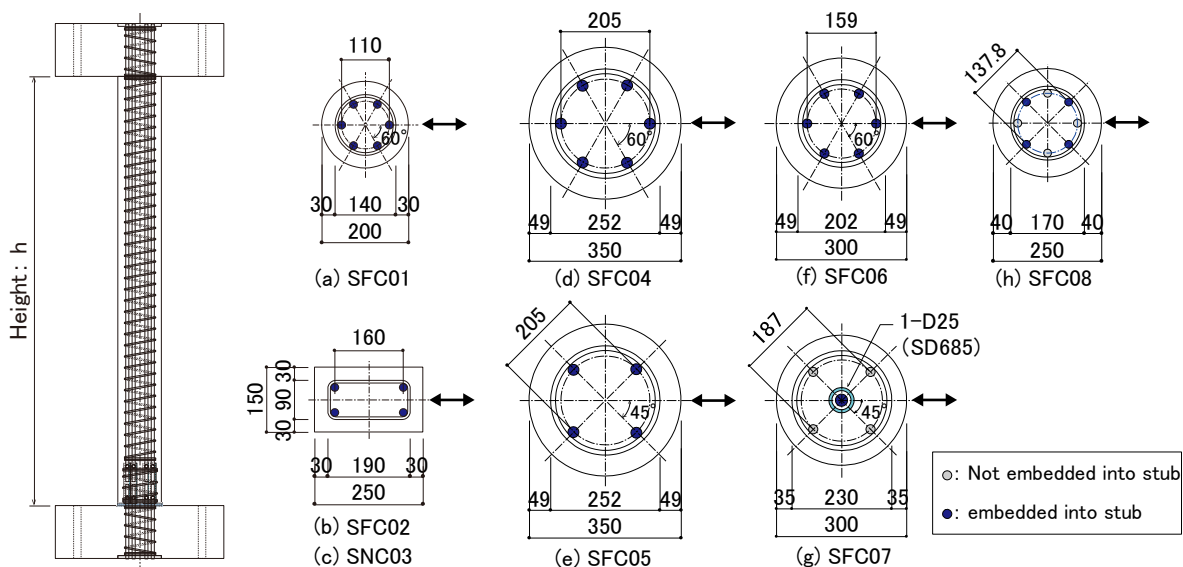


Fig. 3 – Elevation and cross sections of specimens (Unit: mm)

(3) Series 3

In Series 3, the concrete strength of SFC08 was 200 N/mm², the cross section diameter was 250 mm, the main bars were of SD295 type, and the hoops were of SR295 type. The h/D of the column was 9.94. Only four main bars from the eight were embedded into the stub.

2.2 Loading plan

As shown in Fig. 4, experiments were carried out using a pantograph system to apply loading. Specimens were subjected, simultaneously, to axial and lateral loads. Fig. 5 shows the loading history relative to the lateral load. While the axial load was kept constant when testing each specimen, the axial load ratio varied from a specimen to another and ranged from $\eta = 0.25$ to 0.30. The upper part of the loading setup was provided with linear sliders to let the axial force jacks slide when applying the lateral loading. Lateral loading was controlled by displacement where the amplitude was gradually increased starting with the drift ratio $R = 0.1\%$. Taking into account the repeated vibrations caused by long-period ground motions, major drift ratios were repeated 10 times.

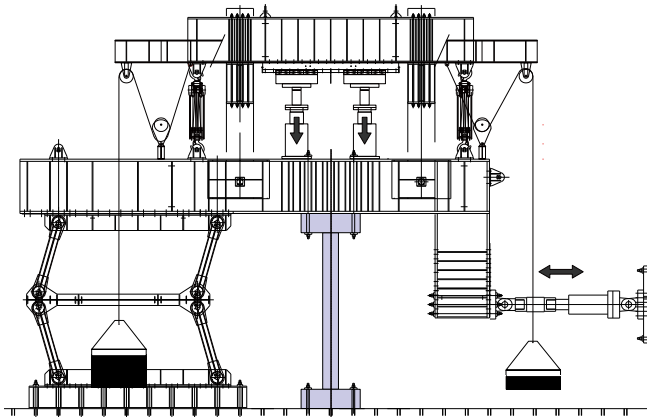


Fig. 4 – Experimental test setup

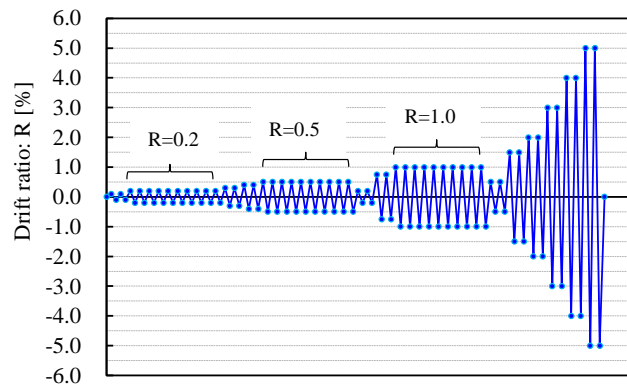


Fig. 5 – Lateral loading history

3. Experimental Results

(1) Series 1

Fig. 6 shows the damage undergone by the specimens of Series 1. Firstly, no damage was observed on all specimens between the drift ratio $R = 0.1\%$ and 0.5% . Between $R = 0.5\%$ and 1.0% , crushing occurred in the grout joints at the base and top ends of columns. At $R=1.0\%$, flexural cracking occurred in the columns at a distance $1.0D$ (D is column depth) from columns' ends. SNC03, which did not contain steel fibers, was damaged at its base corners at the fifth loading cycle of the drift ratio $R = 1.0\%$ when it reached its maximum strength. After that, peeling of cover concrete gradually occurred. At $R = 3.0\%$, the column could no longer hold the applied axial load, after the entire cover concrete had been peeled off. In the contrary, SFC01 and SFC02, which contained steel fibers, were less damaged than SNC03 proving the effectiveness of fibers. Furthermore, although peeling occurred at their base and top ends, these two columns could hold the applied axial forces until the end of testing.

Fig. 7 shows the lateral load - drift ratio relationships and changes of vertical displacements. In the figure, the calculated flexural ultimate strength values based on the ACI Building Code (ACI318)^[8], Standards Association of New Zealand (NZS3101)^[9], and Architectural Institute of Japan (AIJ)^[10] are also shown. The calculated values in the figures considered the reduction due to the P- Δ effect, as the response of such slender columns is considerably sensitive to it. The comparison of the calculated values and experimental results is discussed in the following Chapter 4. Lateral load - drift ratio curves were linear until flexural and compression cracks had

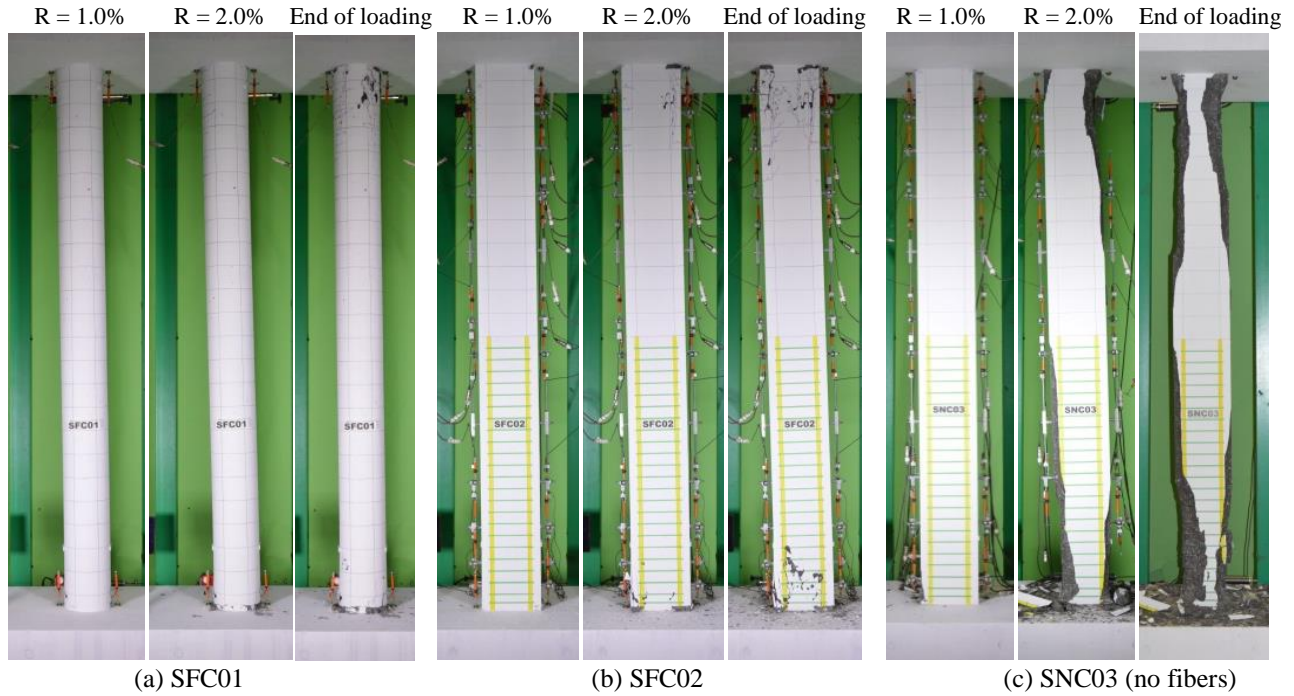


Fig. 6 – Damages of specimens

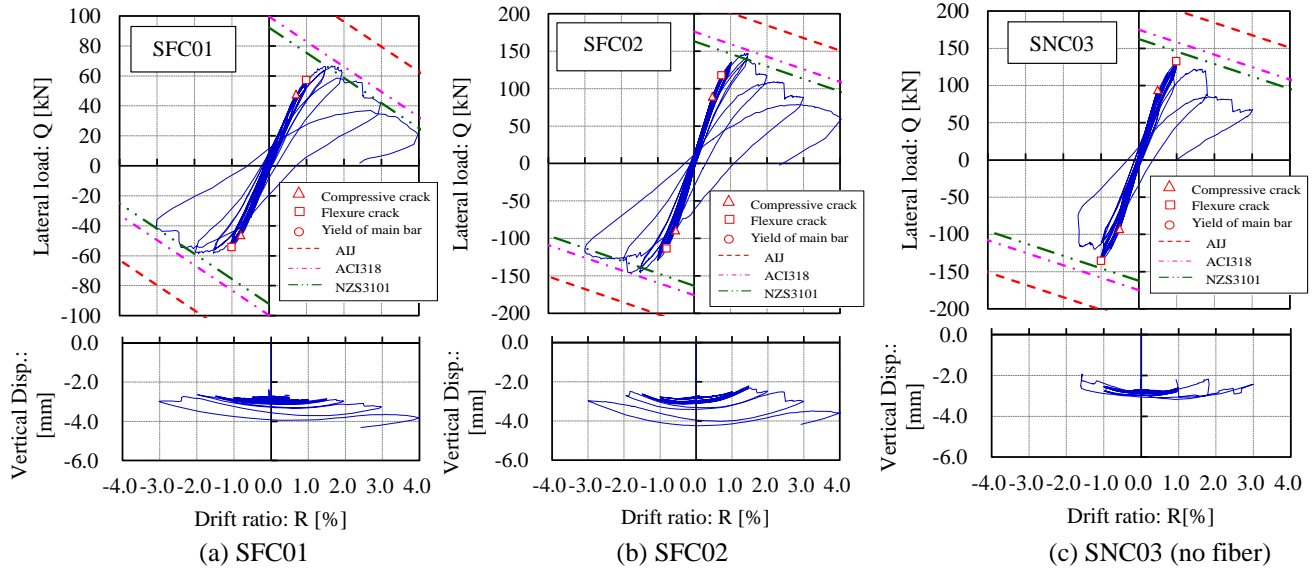


Fig. 7 – Lateral load (Vertical displacement) – Drift ratio relationships

occurred. SFC01 and SFC02 reached their maximum strengths at $R = 1.5\%$. Their ultimate drift ratios (corresponding to 20% decrease in strength after the maximum) slightly exceeded $R = 2.0\%$. As to the vertical displacement - drift ratio relationship, until $R = 1.5\%$ when damage was of minor level, the vertical displacement was about 3.0mm. After the cover concrete of columns' corners was damaged at $R = 4.0\%$, while the vertical displacement exceeded 5.0mm, the columns had enough capacity to hold the applied axial load. While the vertical displacement of SNC03, until $R = 3.0\%$, was similar to those of the other specimens containing steel fibers, since then it had become larger as the column reached its axial bearing capacity.

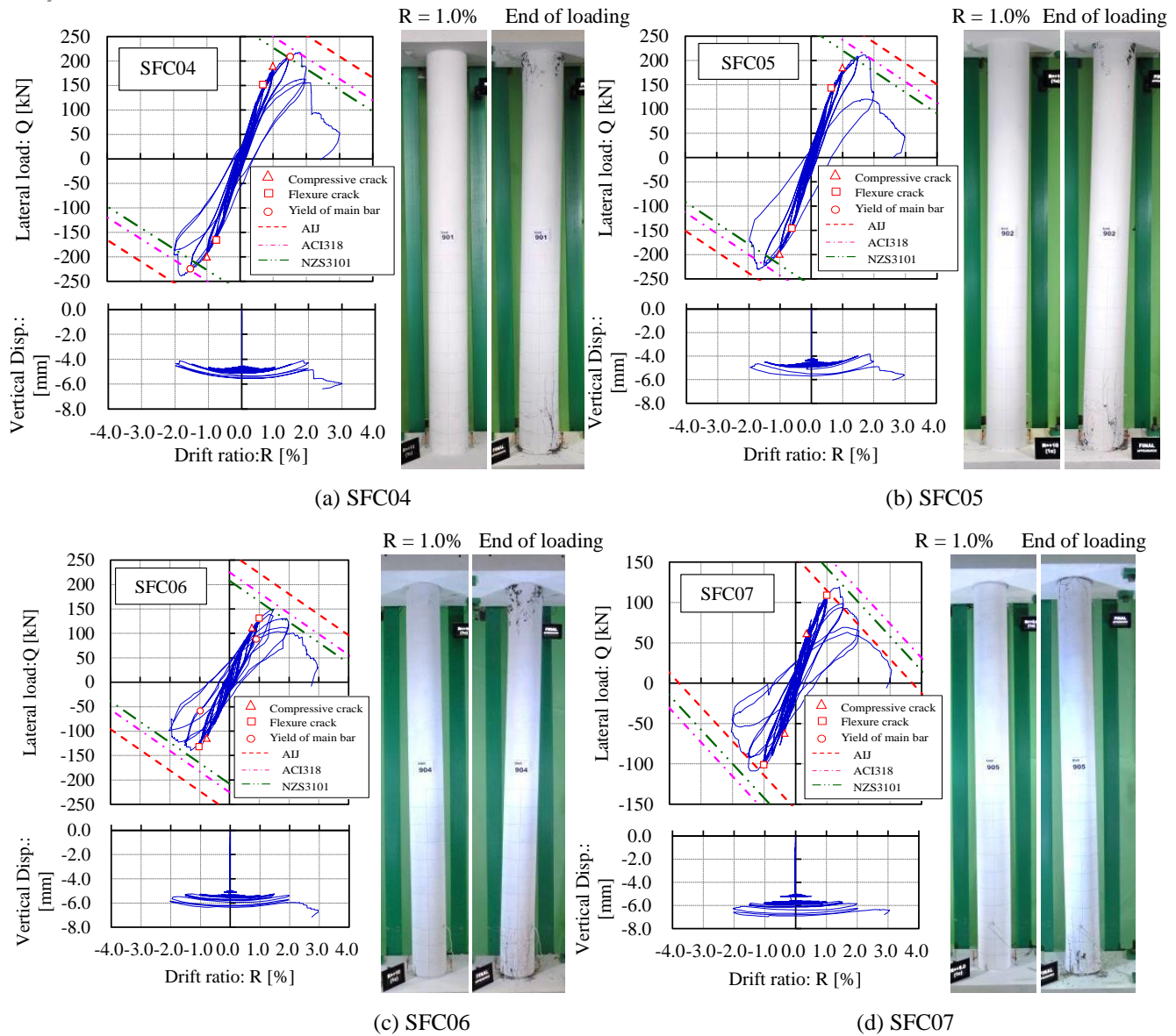


Fig. 8 – Lateral load (Vertical displacement) - Drift ratio relationships and damage of specimens

(2) Series 2

Fig. 8 shows the lateral load - drift ratio relationships of specimens of Series 2 and their respective damages. All specimens experienced cracking at R = 0.7%. Bending cracks occurred at a distance 0.5D from the columns' ends. Slight crushing occurred in the joints at the base and top of columns at R = 1.0%. Main bars of SFC04 experienced compressive yielding at R = 1.5% and the specimen reached its maximum strength at R = 1.9%. SFC05, with less main bars than SFC04, also experienced slight crushing but it was sudden when compared with that of SFC04. This means that the main bars had affected the concrete vertical displacement as they hold a proportion of the compression load. SFC06 made of 200N/mm² concrete experienced rapid crushing of its cover concrete than SFC04. SFC07 showed similar failure type and less strength than SFC06, as the single embedded main bar was centered. For the specimens of Series 2, the vertical displacements were about 6.0mm at the drift ratio of the final loading cycle. These displacements were very small, and in terms of deformation the strains were about 0.17%, which left the specimens with enough capacity to hold the axial load even beyond the ultimate level.

(3) Series 3

Fig. 9 shows the experimental results of SFC08, which contained SD295 main bars and SR295 hoops. Until $R = 1.0\%$, this specimen showed a same behavior as those of other specimens, but at the ultimate level that corresponded to $R = 2.0\%$, it showed an abrupt failure and lost its capacity to hold the applied axial load. At that time, the main bars buckled after experiencing compressive yielding and the hoops ruptured. Therefore, when using ultra-high strength concrete, slender columns would experience fragile failure if high strength reinforcement were not adopted.

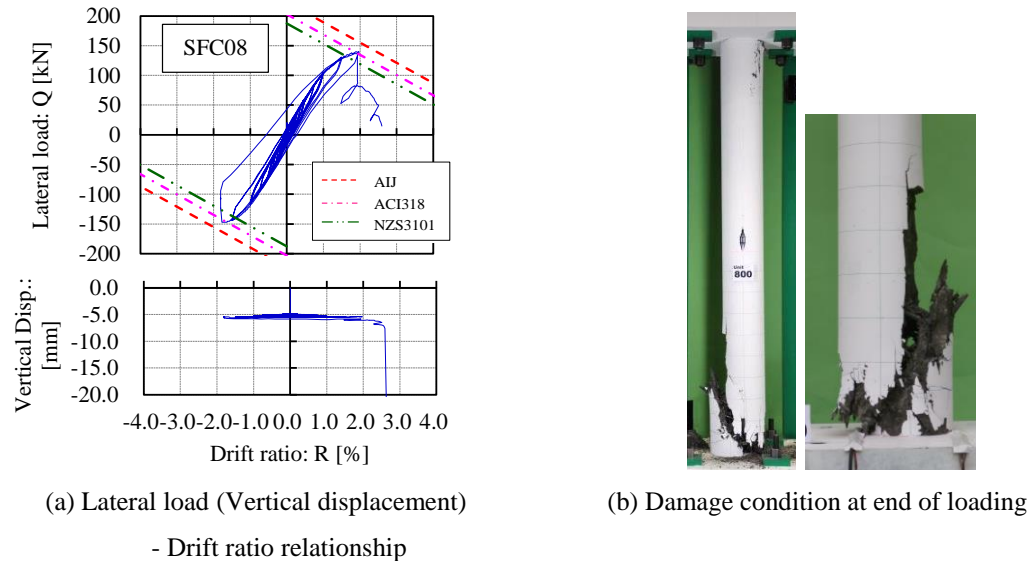


Fig. 9 – Experiment results of SFC08

4. Consideration of Experiment

4.1 Effect of steel fibers

Fig. 10 shows damage comparison of SFC02 and SNC03 at $R = 1.5\%$. SFC02, which contained mixed steel fibers, showed less damage than SNC03, which did not contain steel fibers. Fig. 11 shows a comparison between the lateral - drift ratio curves of the two specimens. SNC03 experienced start of crushing and peeling of cover concrete simultaneously, and when the cover concrete was entirely peeled off at $R = 1.0\%$, the specimen reached its maximum strength, which was 0.90 times that of SFC02. Because of the absence of steel fibers in SNC03, an early rupture occurred along the interface between the core concrete and cover concrete on the compression side of the column section due to bending moment. Fig. 12 shows the effect of fiber reinforcement from four-point bending tests that were carried out on $100 \times 100 \times 400$ mm prism specimens. These tests showed that toughness of high-strength concrete was enhanced by the addition of steel fibers, which explained the solid behavior of the cover section and core section of SFC02. Therefore, it was deduced that by controlling the rupture of cover concrete, it would be possible to evaluate the previously tested columns using the existing design equations.



(a) SFC02 (mixed fibers) (b) SNC03 (no fibers)

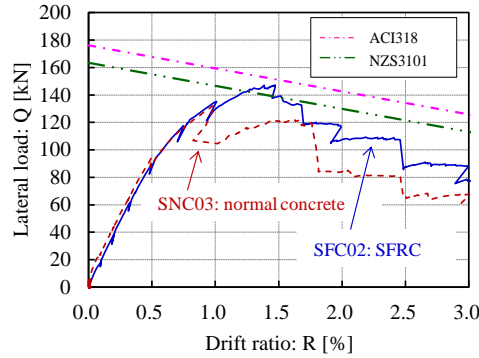


Fig. 10 – Comparison of specimens

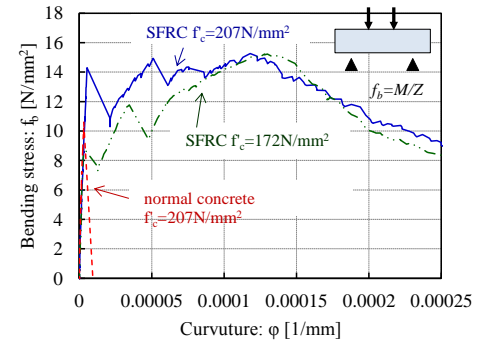


Fig. 11 – results of bending test on prisms

4.2 Comparison of test flexural strengths and calculated values

Experimental maximum strengths were compared with the calculated values in terms of the ultimate flexural strength using the design standards ACI318^[8], NZS3101^[9] and AIJ^[10], as listed in Table 2. The values of Q'_{max} given in Table 2 were calculated taking into account the $P\Delta$ effect. To evaluate the specimens, the cross sections of the circular columns were replaced by equivalent square cross sections of the same areas. Furthermore, when the main bars were not embedded into the stubs, they were not considered in the calculations either for compression or tension. Material properties obtained from material tests were used in the calculations. As a representative method of the three used standards, the calculation method of flexural ultimate strength using the stress block of NZS3101 is shown by equation (1), while its corresponding stress block is shown in Fig. 13. While the factor α_1 of the stress block is commonly taken as 0.85 in ACI318, in NZS3101, for high strength concrete, it is reduced from 0.85 to 0.65 in accordance to the strength of concrete. The stress-strain relationship of high strength concrete is simulated by a linear curve and the stress state is considered of triangular shape. Fig. 14 shows the calculated $Q-N$ interaction curves of SFC02 based on the three standards. Calculation by AIJ overestimated the strength of the specimens, because the applied axial load was close to axial load relative to the balanced state given in the standard. Values by ACI318 and NZ3101 were approximately equal to the experimental results.

Table 2 – Comparison of flexural strengths with calculated values

Specimen	Experimental value			Calculated Value			Exp. / Cal.		
	Drift ratio at maximum load: R_{max} [%]	Maximum load: Q_{max} [kN]	Corrected Maximum load: Q'_{max} [kN]	ACI318 Q_{aci} [kN]	NZS3101 Q_{nzs} [kN]	AIJ Q_{aij} [kN]	ACI318 Q'_{max} / Q_{aci}	NZS3101 Q'_{max} / Q_{nzs}	AIJ Q'_{max} / Q_{aij}
SFC01	16.8	67	96	100	92	130	0.96	1.04	0.74
SFC02	14.7	147	177	175	162	218	1.01	1.09	0.81
SNC03	10.0	132	155	184	171	222	0.84	0.90	0.70
SFC04	17.6	222	295	293	271	339	1.01	1.09	0.87
SFC05	16.2	216	286	285	265	324	1.00	1.08	0.88
SFC06	14.9	150	213	225	208	265	0.95	1.03	0.80
SFC07	13.9	119	178	216	200	178	0.83	0.89	1.00
SFC08	18.7	140	207	203	188	224	1.02	1.11	0.93

NZS3101

$$M_u = \sum A_{st} \cdot f_{st} \cdot d - \sum A_{sc} \cdot f_{sc} \cdot d_c - \alpha_1 \cdot f'_c \cdot b (\beta_1 \cdot x_n)^2 / 2 + N \cdot g \quad (1)$$

$$\alpha_1 = \begin{cases} 0.85 & (f'_c < 55.0) \\ 0.85 - 0.004(f_c - 55) & \alpha_1 \geq 0.75 \quad (f'_c \geq 55.0) \end{cases} \quad \beta_1 = \begin{cases} 0.85 & (f'_c \leq 27.5) \\ 0.85 - 0.51(f'_c - 27.5) / 70 & (27.5 < f'_c \leq 55.0) \\ 0.65 & (55.0 < f'_c) \end{cases}$$

A_{st} : Crosssectional area of tensile main bar, f_{st} : Yield strength of main bar, d : Distance of column depth
 A_{sc} : Crosssectional area of compressive main bar, f_{sc} : Yield strength of main bar, d_c : Distance of Compressive main bar
 g : Centroid position, f'_c : Concrete strength, b : width of section
 x_n : neutral position, N : Axial force

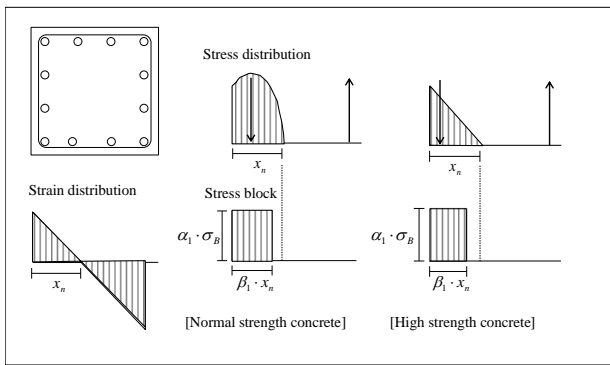


Fig. 13 – Stress block of NZS3101 standard

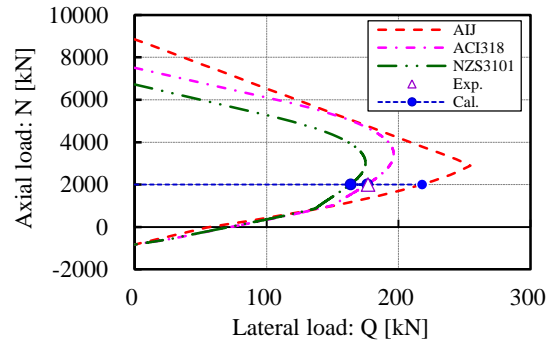


Fig. 14 – Q-N interaction curve (SFC02)

Fig. 15 shows the correlations between the experimental results and calculated values. The mean ratio of the calculated values by ACI318 to the experimental results was 0.96, and the coefficient of variation (CV) is 6.4%. The mean ratio of the calculated values by NZS3101 was 1.03, and CV was 6.5%. The mean ratio of the calculated values by AIJ was 0.86, and CV was 14.8%. While the calculated values by AIJ overestimated the strengths, those calculated by NZS3101 were substantially lower than the experimental values on the safe side. Therefore, for the evaluation of high strength SFRC slender columns, the stress block of NZS3101 would be suitable.

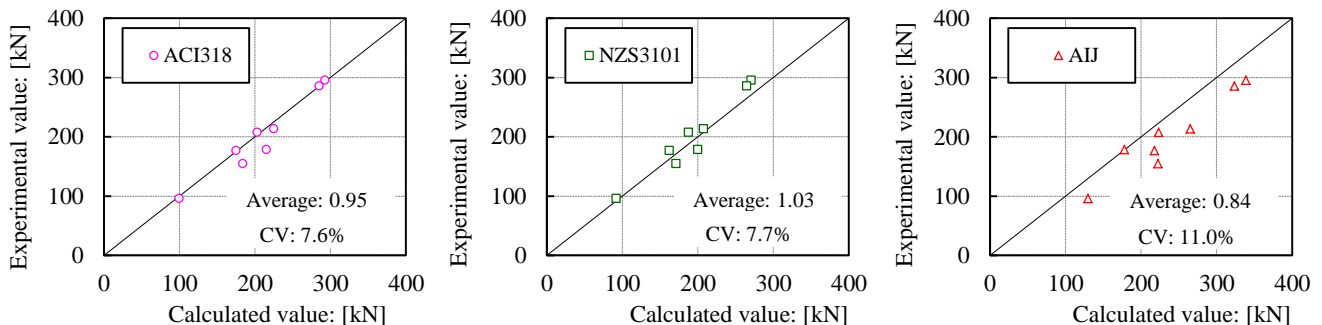


Fig. 15 – Correlations between experimental results and calculated values



5. Conclusion

Experimental study was carried out on slender columns made with SFRC of compressive strength ranging from 172 to 234 N/mm². Two types of fibers were mixed into the concrete of seven specimens, while only one specimen did not contain fibers. The tested columns were subjected to combined axial compression and lateral loading. The following findings were drawn.

- 1) Structural properties of the tested high strength SFRC slender columns were obtained. The dominant failure mode of the specimens was of flexural compression type, except the specimen with normal strength reinforcement bars, which experienced a fragile failure mode. The failure occurred at the column base of all specimens.
- 2) High strength steel type should be used as longitudinal reinforcement to prevent fragile failure mode.
- 3) Specimens containing steel fibers, showed a better seismic performance than specimens without steel fibers.
- 4) Specimens containing steel fibers did not experience spalling of concrete cover and, consequently, had enough capacity to hold the axial load until about R=3.0%, without a sign of degradation in the loading bearing capacity. In the contrary, the specimen without steel fibers showed large damage. It experienced peeling of cover concrete portion and, consequently, showed a loss of the loading bearing capacity at R=3.0%. The loss of concrete cover affected also the lateral capacity of the specimen, where the maximum strength was 10% lower than that of the columns with steel fibers.
- 5) A comparison between the experimental results and flexural calculated values of ACI318, NZS3101, and AIJ was made. Calculated values of AIJ overestimated the strength of tested columns. Using the stress block of NZS3101 resulted in calculated strength values that agreed well with experiment results, and were on the safe side.
- 6) Restoring force characteristics of high strength SFRC slender columns will be examined in a future study.

6. References

- [1] Fafitis and Shah: Lateral Reinforcement for High-Strength Concrete Columns, ACI, No.SP-87, pp.213-232, 1985
- [2] Mark Fintel, et al., Column Shortening in Tall Structures, Portland Cement Associations, 1986
- [3] The world's highest building is taking shape, Engineers AUSTRALIA Vol.79, No.2, 2007
- [4] Michel P. Collins, et al. , Structural Design Considerations for High-Strength Concrete, Concrete International, pp.27-34, 1993, ACI
- [5] T. Nagashima, S. Sugano, H. Kimura, A. Ichikawa: Monotonic Axial Compression Test on Ultra-High-Strength Concrete Tied Columns, 10th World Conference on Earthquake Engineering, pp.2983-2988, 1992
- [6] F. Tomosawa, T. Noguchi, Relationship between Compressive Strength and Modulus of Elasticity of High-Strength Concrete, High-Strength Concrete, Third International Symposium, pp.1247-1254, 1993
- [7] Y. Sun, K. Sakino, Flexural Behavior of Reinforced Concrete Columns Confined in Square Steel Tube, 10th World Conference on Earthquake Engineering, pp.4365-4370, 1993
- [8] American Concrete Institute: Building Code Requirements for Structural Concrete (ACI318-14) and Commentary, 2014
- [9] Standards Association of New Zealand: Concrete Design Standards, NZS3101, 2011.
- [10] Architectural Institute of Japan (AIJ), Ultimate Strength and Deformation Capacity of Buildings in Seismic Design (1990), 1990
- [11] Togay Ozbakkaloglu, Murat Sattcioglu, Rectangular Stress Block for High-Strength Concrete, ACI Structural Journal, Vol.101, No.4, pp.475-483, 2004